tween 20,000 and 75,000 ft for several areas in the northern hemisphere," NASA TN D-548 (1960).

[2] Taback, I., "The NACA oil-damped V-G recorder," NACA TN 2194 (1950).

[3] Richardson, N. R., "NACA VGH recorder," NACA TN 2265 (1951).

[4] "The thunderstorm: report of the thunderstorm project," Weather Bureau, U. S. Dept. of Commerce, Washington, D. C. (June 1949).

[5] Staff, "National severe storms project objectives and basic design," Rept. 1, National Severe Storms Project, Weather Bureau, U. S. Dept. of Commerce, Washington, D. C. (March 1961).

[6] Press, H. and Steiner, R., "An approach to the problem of estimating severe and repeated gust loads for missile operations," NACA TN 4332 (1958).

[7] Pratt, K. G. and Walker, W. G., "A revised gust-load formula and a re-evaluation of V-G data taken on civil transport airplanes from 1933 to 1950," NACA Rept. 1206 (1954).

[8] Notess, C. B., "The effects of atmospheric turbulence upon flight at low altitude and high speed," Frequency Div. Multiplex 325, Cornell Aeronautical Lab., Inc. (October 31, 1961).

[9] Rhyne, R. H. and Steiner, R., "Power spectral measurement of atmospheric turbulence in severe storms and cumulus clouds," NASA TN D-2469 (1964).

JAN.-FEB. 1966 J. AIRCRAFT VOL. 3, NO. 1

Parachute Stress Analysis during Inflation and at Steady State

H. G. Heinrich*
University of Minnesota, Minneapolis, Minn.

AND

L. R. Jamison Jr.†
Pioneer Parachute Company, Manchester, Conn.

The stresses occurring in the cloth of a parachute during the period of inflation and at steady state are calculated for a number of instantaneous shapes that are characteristic of the opening process and the steady state. The method is general and may be applied to any type of parachute built out of solid cloth, concentric rings, or ribbons. The presented analysis is related to canopies consisting of triangular gores but can be extended to other gore patterns. A numerical calculation is made for a solid flat circular parachute during the period of opening and at steady state.

Nomenclature

b_0 = a length (Figs. 4 and 5)
C_p = pressure coefficient
D = projected diameter
D_0 = canopy nominal diameter
D_v = vent diameter
d_0 = a length (Fig. 5)
E = cloth modulus of elasticity, lb/ft
f_1 = circumferential stress (Fig. 2), lb/ft
f_2 = meridional stress (Fig. 2), lb/ft
F = force between canopy and store (Fig. 4)
F_{max} = opening force or opening shock
N = number of gores
plane Q = illustrated in Fig. 4
Δp = pressure differential across cloth (Fig. 5)
q = dynamic pressure $\equiv \frac{1}{2}\rho V^2$
r_b = bulge radius (Figs. 2 and 5)
S = area
S_0 = canopy nominal area
s = a length (Figs. 2 and 6)
t = time
t_f = filling time
V = velocity
V_0 = initial velocity
W_s = store weight
x = a length (Figs. 2 and 4)
y = a length (Fig. 5)
z = a length (Fig. 4)
α = gore half-angle (Fig. 5)
ϵ = strain
θ = angle between suspension lines and canopy centerline (Fig. 4)
λ^* = a dimensionless parameter [Eq. (23)]
ρ = radius of curvature (Fig. 2)
ϕ = an angle (Fig. 4)

Superscript

$*$ = a dimensionless quantity

Subscripts

0 = initial or unstretched condition
c = referred to cord line
g = referred to gore centerline
∞ = freestream conditions

Presented at the AIAA Entry Technology Conference, Williamsburg, Va., October 12–14, 1964 (no preprint number; published in bound volume of preprints of the meeting); revision received April 1, 1965. The work has been sponsored jointly by the U. S. Army, Air Force, and Navy under Contract No. AF 33(657)-11184. The authors wish to express their gratitude to the students of Aerospace Engineering who participated in this study, particularly to Daryl J. Monson.

* Professor of Aeronautical Engineering. Associate Fellow Member AIAA.

† Senior Analyst.

I. Introduction

THE known analytical studies of parachute stresses are primarily concerned with the steady-state phase, during which the drag of the parachute equals the suspended weight. The earliest studies of the canopy stresses have been summarized by Jones in 1923,[1] and they consider the canopy shapes and stresses under the assumption of an infinite number of gores.

In 1942, Stevens and Johns[2] introduced into the basic analysis the concept of a finite number of gores and also

showed that the stresses in the cloth are only circumferential. This agrees with the later analysis by Duncan, Stevens, and Richards,[3] which furthermore utilized the elasticity of the cloth in order to encompass the stresses at the apex.

Beck[4] assumed that inflated parachute canopies are surfaces of revolution and derived for this case expressions for the stresses considering constant and varying differential pressures. Reagan[5] also considered parachutes as surfaces of revolution.

Newer studies by Topping, Marketos, and Costakos[6] pursue a solution for the cloth stresses of a fully inflated canopy on the basis of a calculated canopy profile. This profile is obtained from the so-called Taylor curve[1] and a correction in view of actual gore patterns. This method provides the characteristic bulging of the material between adjacent suspension lines. Canopy profiles are calculated in this manner and agree with experimentally obtained canopy shapes within 4 to 9%.[6] Stresses are then determined for the calculated canopy profiles.

The following stress analysis assumes that the canopy profile of the fully inflated parachute is either known or can be obtained from full-size or model experiments. The stresses can then be calculated in view of the known profile, the given gore pattern, and the experimentally determined pressure distribution.

Furthermore, this method is expended to cover the period of canopy inflation, and for this phase intermediate canopy shapes are assumed, as proposed by O'Hara.[7] Coupled with the stress analysis is the calculation of the parachute opening force, which provides the instantaneous values of the pressure differential that acts upon the canopy cloth.

II. Canopy Profile

The gores of a parachute during inflation and at steady state bulge out between adjacent cord lines, and the first step in the stress analysis in the establishment of the gore and cord profiles. In principle, merely one needs to be known, and the other can be calculated by means of the related gore pattern.

Adopting for the period of inflation the schematic-canopy shapes as proposed by O'Hara,[7] one may establish a number of characteristic profiles, as shown in Fig. 1. The outline of

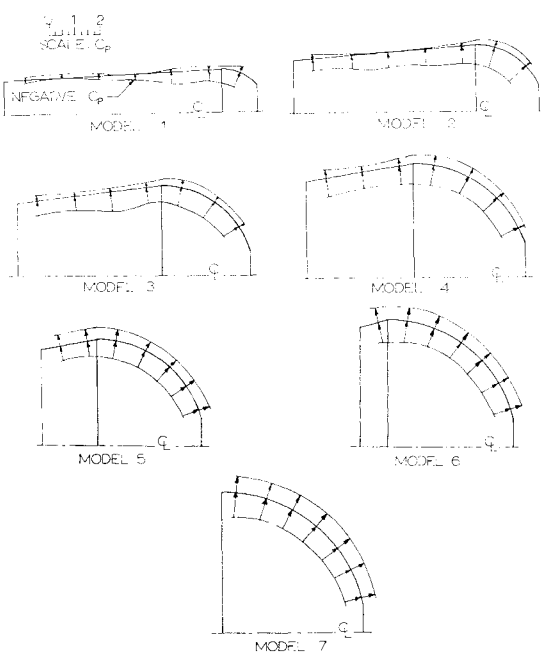

Fig. 1 Characteristic shapes representing an inflating canopy and related pressure distributions.

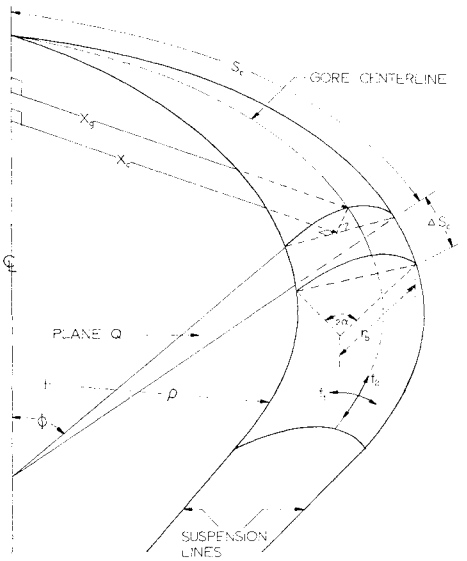

Fig. 2 Orientation of a gore element.

these figures may be considered as cord profiles. Superimposed upon these profiles is a pressure distribution that was obtained through wind-tunnel experiments.[8] These pressure distributions will be needed later for the actual calculation of the canopy stresses. Proceeding in this manner, the form of the parachute under steady-state descent becomes merely a special case, which is somewhat identical to model 7, Fig. 1.

The stress in various sections of the canopy depends now on the instantaneous shape and the respective pressure differential and will be determined in view of the following simplifying assumptions:

1) At any instant of opening and at steady state, the pressure loading is constant circumferentially but varies in the meridional direction.

2) The resultant stress in a gore element extending between adjacent suspension lines is primarily circumferential.

3) The cross-sectional shape in a plane Q (Fig. 2) of any gore element is a circular arc because of uniform pressure distribution over the element and cannot exceed a semicircle. In case of excess cloth, the particular cross section is treated as a semicircle with parallel extensions to the cord.

4) Inertial forces and the related stresses in the gore element which may occur during inflation are neglected.

5) Details of the canopy geometry are shown in Figs. 2–6.

III. Cord-Line Profile

One may proceed to determine the cord profile from a known gore profile or vice versa. Following the traditional approach, the cord profile will be determined from a known gore profile.

In the first approximation, the cloth and cords are considered to be inextensible. All values obtained under this

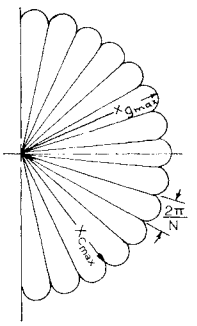

Fig. 3 Canopy plan view.

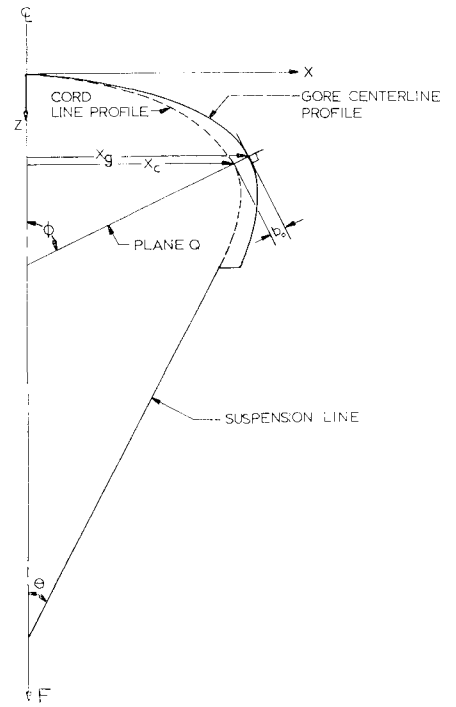

Fig. 4 Profile view of a parachute canopy.

condition are identified by the subscript zero. The elasticity of the cloth will be introduced later.

As a first step in the analysis, the length b_0, as shown in Figs. 4 and 5, will be expressed in terms of known quantities. This will allow the determination of the cord profile, since b_0 is measured to the gore centerline.

From Fig. 5 follows

$$y = 2r_{b_0}\sin\alpha_0 = 2r_{b_0}[\alpha_0 - (\alpha_0^3/3!) + \ldots] \quad (1)$$

and

$$d_0 = 2r_{b_0}\alpha_0 \quad (2)$$

In addition, it may be written that

$$b_0 = r_{b_0}(1 - \cos\alpha_0) = r_{b_0}[1 - 1 + (\alpha_0^2/2!) - (\alpha_0^4/4!) + \ldots] \quad (3)$$

In Eqs. (1) and (3), $\sin\alpha_0$ and $\cos\alpha_0$ have been expanded in series form. This form is very convenient, and sufficient accuracy is maintained with the indicated terms.

A typical flat gore is shown in Fig. 6, for which one sets

$$d_0 = 2s_g\tan(\pi/N) \quad (4)$$

where N is the number of gores.

Also, from Figs. 2, 4, and 5 it can be seen that

$$y = 2x_c\tan(\pi/N) \quad (5)$$

In view of the basic concept, namely, that merely the profile of the gore centerline is known, the term x_c in Eq. (5) is unknown, and a further relation is necessary.

From Figs. 2 and 4 follows

$$x_c = x_g - b_0\sin\phi \quad (6)$$

These six equations contain the six unknowns y, r_{b_0}, α_0, b_0, d_0, and x_c, whereas the quantities N, x_g, s_g, and ϕ are known, and the equations can be solved for b_0 and for r_{b_0}, which are sufficient to determine the stress.

It has been found, however, that the equation for b_0 becomes very cumbersome when expressed in the known terms of x_g and s_g. The solution in terms of x_c and s_g is much simpler, and, after some algebraic manipulations, one obtains

$$b_0 = [\tan(\pi/N)/4]\{6[1 - (x_c/s_g)]\}^{1/2}(s_g + x_c) \quad (7)$$

This equation includes the unknown term x_c. However, it will be seen that for most practical cases $x_c \approx x_g$, and if this is unsatisfactory a certain iteration process can be performed which quickly converges. Details of this matter will be discussed at the end of this section.

Equation (7) is valid as long as the gore element forms an arc equal to or less than a semicircle. When the gore bulges in the shape of a semicircle with parallel extension, the geometry of Fig. 5 indicates that

$$b_0 = \frac{y}{2} + \frac{1}{2}\left(d_0 - \frac{\pi}{2}y\right) = \frac{1}{2}\left[d_0 + \left(1 - \frac{\pi}{2}\right)y\right] = \tan\frac{\pi}{N}\left[s_g + \left(1 - \frac{\pi}{2}\right)x_c\right] \quad (8)$$

where the last step results from substitution of Eqs. (4) and (5). Finally, expressing b_0 in terms of x_g and s_g by means of Eq. (6) gives

$$b_0 = \frac{\tan(\pi/N)\{s_g + [1 - (\pi/2)]x_g\}}{1 + \tan(\pi/N)[1 - (\pi/2)]\sin\phi} \quad (9)$$

For the practical stress solution, one must determine which equation for b_0 has to be used. For this purpose, the following criterion will be established. Figure 5 shows that an arc less than a semicircle occurs if

$$d_0 < (\pi/2)y \quad (10)$$

Substitution of Eqs. (4) and (5) for d_0 and y gives inequality (10) as

$$2s_g/\pi x_c < 1 \quad (11)$$

The term x_c may be replaced by Eq. (6) to give

$$2s_g/[\pi(x_g - b_0\sin\phi)] < 1 \quad (11a)$$

Therefore, if the actual conditions satisfy Eq. (11a), b_0 must be calculated from Eq. (7).

Equation (11a) indicates that, if the inequality is reversed to

$$2s_g/[\pi(x_g - b_0\sin\phi)] \geq 1 \quad (12)$$

and the actual conditions satisfy this equation, b_0 should be calculated from Eq. (9).

Substituting b_0 by means of Eq. (9) into Eq. (12) gives, after some manipulation,

$$\frac{(2s_g/\pi)\{1 + \tan(\pi/N)\sin[\phi 1 - (\pi/2)]\}}{x_g - \sin\phi\tan(\pi/N)s_g} \quad (13)$$

This is now an expression of known quantities, and, in summary, it may be stated that b_0 should be calculated in

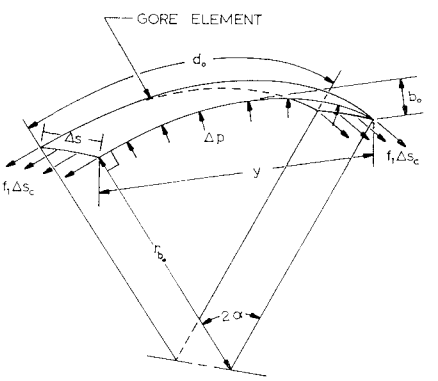

Fig. 5 Gore and cord-line element with applied forces.

accordance with the following criterion:

$$\left|\frac{(2s_g/\pi)\{1 + \tan(\pi/N)\sin\phi[1 - (\pi/2)]\}}{x_g - \sin\phi\tan(\pi/N)s_g}\right| \begin{cases} < 1, \text{ apply Eq. (7)} \\ \geq 1, \text{ apply Eq. (9)} \end{cases} \quad (14)$$

The preceding equations become more universal in dimensionless form by means of the nominal parachute diameter, D_0, and one obtains

$$b_0^* = b_0/(D_0/2) \qquad x_c^* = x_c/(D_0/2) \qquad s_c^* = s_c/(D_0/2)$$

$$x_g^* = x_g/(D_0/2) \qquad s_g^* = s_g/(D_0/2) \quad (15)$$

In these terms, Eqs. (6, 7, 9, and 14) assume the form of

$$b_0^* = \frac{\tan(\pi/N)}{4}\left[6\left(1 - \frac{x_c^*}{s_g^*}\right)\right]^{1/2}(s_g^* + x_c^*) \quad (7a)$$

$$x_c^* = x_g^* - b_0^*\sin\phi \quad (6a)$$

$$b_0^* = \frac{\tan(\pi/N)\{s_g^* + [1 - (\pi/2)]x_g^*\}}{1 + \tan(\pi/N)[1 - (\pi/2)]\sin\phi} \quad (9a)$$

and the criterion is

$$\left|\frac{2s_g^*\{1 + \tan(\pi/N)\sin\phi[1 - (\pi/2)]\}}{x_g^* - s_g^*\sin\phi\tan(\pi/N)}\right| \begin{cases} < 1, \text{ apply Eq. (7a)} \\ \geq 1, \text{ apply Eq. (9a)} \end{cases} \quad (14a)$$

The actual procedure to find the significant canopy parameters that ultimately will lead to the determination of the stress distribution may now be described as follows:

1) Establish from available photographs or by other means the profile of the gore centerline.

2) Erect at several values of s_g^* the normal to the gore-centerline profile, and extend these lines to the canopy centerline. These lines are the traces of the planes Q, as shown in Figs. 2 and 4.

3) Determine the distances x_g^* and s_g^* and the angle ϕ related to each value of s_g^* on the gore centerline.

4) Determine which equation for b_0^* applies from inequality (14a).

5) Calculate b_0^* from either Eq. (7a) or Eq. (9a). If Eq. (7a) is used, calculate a first approximation for b_0^* by using x_g^* in place of x_c^*. The accuracy of this interchange depends on the included angle of the gore, which in turn is a function of the parachute diameter and its number of gores. If better accuracy is needed, the first approximation for b_0^* can be used in Eq. (6a) to find x_c^*. By using Eqs. (6a) and (7a) in this manner, an iteration process can be applied until a value for b_0^* is obtained which satisfies both equations.

6) Lay off the final values for b_0^* in the planes Q and construct the cord-line profiles.

These steps complete the canopy geometry.

IV. Cloth Stresses

The basic equation relating cloth stress to the pressure differential and the gore bulge is[8]

$$f_1 = \Delta p r_b \quad (16)$$

In order to obtain the cord-line profile, the cloth was assumed inextensible. This requirement is now removed, and it will be assumed that the cloth is perfectly elastic, obeying Hook's Law, which provides

$$f_1 = E\epsilon \quad (17)$$

It is known, however, that parachute cloth, particularly nylon material, deviates from this ideal behavior. But for simplicity, E may be taken in the first approximation as a constant, equal to the ratio of the failure stress to the related strain.

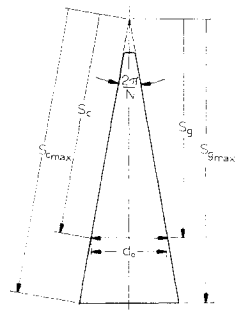

Fig. 6 Triangular gore pattern for a solid flat canopy.

If it can be assumed that the strain is constant over any gore element, one may write from the conventional definition of strain and from observation of Figs. 5 and 6 that

$$\epsilon = \Delta d/d_0 = (d - d_0)/d_0, \text{ or}$$

$$d = (1 + \epsilon)d_0 \quad (18)$$

Equations (16–18), in addition to the previously derived Eqs. (1) and (2), constitute a system of equations with the unknowns f_1, r_b, α, d, and ϵ. In Eqs. (1) and (2) the subscript zero is now removed, since the cloth is assumed to be elastic.

A solution of the five equations for the stress provides

$$f_1^3 + \left[\frac{6E^3[1 - (x_c/s_g)] - 3E[\Delta p s_g \tan(\pi/N)]^2}{6E^2 - [\Delta p s_g \tan(\pi/N)]^2}\right]f_1^2 - \left[\frac{3E^2[\Delta p s_g \tan(\pi/N)]^2}{6E^2 - [\Delta p s_g \tan(\pi/N)]^2}\right]f_1 - \left[\frac{E^3[\Delta p s_g \tan(\pi/N)]^2}{6E^2 - [\Delta p s_g \tan(\pi/N)]^2}\right] = 0 \quad (19)$$

Equation (19) is valid only as long as $\alpha < 90°$. If stress and strain can be calculated as hoop stress of a semicircle,

$$f_1 = \Delta p x_c \tan(\pi/N) \quad (20)$$

In dimensionless form, these equations are easier to apply. For this purpose, the stress can be expressed by means of the strain from Eq. (17), and all length terms can be divided by D_0. Furthermore, by reviewing Eq. (19), one observes a common group of terms in the coefficients, and it is useful at this time to introduce a dimensionless term λ^*, defined as

$$\lambda^* = \Delta p[(D_0/2)/E]\tan(\pi/N) \quad (21)$$

The nominal diameter D_0 arises in Eq. (21) because of its introduction into Eq. (19) in order to nondimensionalize all lengths.

Substitution of Eqs. (15, 17, and 21) into Eqs. (19) and (20) gives, respectively,

$$\epsilon^3 + \left[\frac{6[1 - (x_c^* s_g^*)] - 3(\lambda^* s_g^*)^2}{6 - (\lambda^* s_g^*)^2}\right]\epsilon^2 - \left[\frac{3(\lambda^* s_g^*)^2}{6 - (\lambda^* s_g^*)^2}\right]\epsilon - \left[\frac{(\lambda^* s_g^*)^2}{6 - (\lambda^* s_g^*)^2}\right] = 0 \quad (19a)$$

$$\epsilon = \lambda^* x_c^* \quad (20a)$$

Now one observes that the design characteristics of the parachute appear in Eqs. (19a) and (20a) only through the dimensionless parameter λ^*. This makes it possible to obtain for any given canopy shape a family of ϵ vs s_g^* curves with λ^* as a parameter. This indicates that for a given parachute type, such as the solid flat parachute, any combination of parachute characteristics resulting in the same value of λ^* will give the same strain-length relationship, ϵ vs s_g^*.

This statement, however, includes also the requirement for identical gore centerline profiles, which, for example, could be altered in spite of identical gore patterns through a variation of the relative length of the suspension lines. The

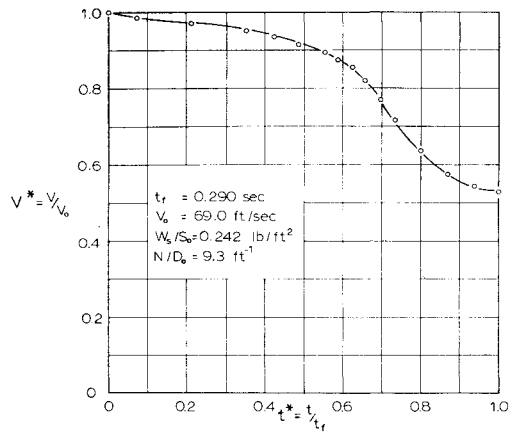

Fig. 7 Velocity-time relationship for an opening solid flat canopy.

parameter λ^* includes the pressure differential Δp, and for the further treatment this term must be determined.

Because of its complexity, the possibility of an analytical determination of the flow pattern, particularly during inflation, must be disregarded at this time. Experimentally, the pressure distribution could be measured by means of transducers that could be attached at various locations to the canopy. However, to date no pertinent information is available.

Another possibility is to find experimentally the pressure distribution of intermediate shapes that are characteristic for the opening process. Such shapes were mentioned before and are shown in Fig. 1. The pressure distribution is given in the form of the pressure coefficient C_p, which is defined as

$$C_p = (p_{\text{local}} - p_\infty)/q_\infty \tag{22}$$

where q_∞ is the dynamic pressure.

In order to find the magnitude of the pressure differential of the inflating canopy, it is now necessary to establish the relationship between freestream velocity and the related projected diameter. This can be obtained from a simultaneously performed opening shock calculation or from an experimentally established velocity-shape-time relationship. In this study, experimental data as illustrated in Figs. 7 and 8 will be used for reasons of simplicity.

It should be realized that the method as just described probably neglects a number of facts that may be connected with the dynamics of the opening process. However, one may assume that, even when a more sophisticated method

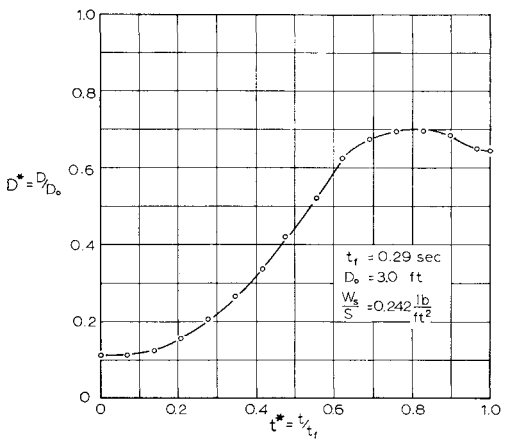

Fig. 8 Diameter-time relationship for an opening solid flat canopy.

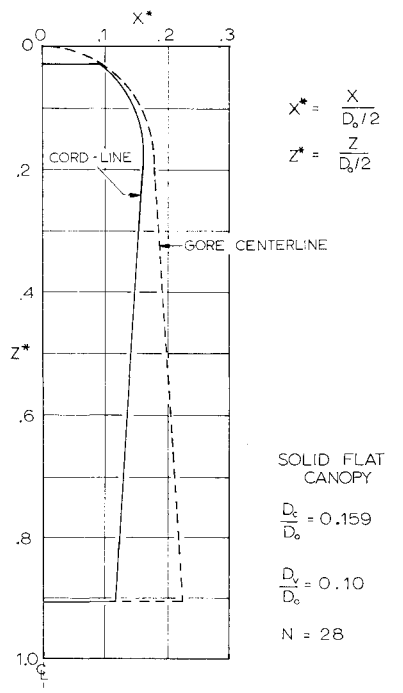

Fig. 9 Profile shape of rigid model 1.

becomes available, the present analysis will be a part of the general calculation.

After this preparation, λ^* can be determined. With this complete, the following steps may be followed to obtain a numerical solution, first of the strain and then of the stress:

1) It is assumed that the cord-line and the gore-centerline profiles are known for different stages of opening. The first step, then, is to determine λ^* for selected values of x_c^* and s_g^*.

2) From Eq. (14a), determine whether α is less than or equal to 90°, which determines whether or not the strain ϵ will be calculated from Eq. (19a) or Eq. (20a), respectively.

3) Equation (19a) could be solved by means of methods for the solution of cubic equations. However, this is cumbersome, and an iteration process leads more quickly to satisfactory results. Equation (20a) indicates the order of

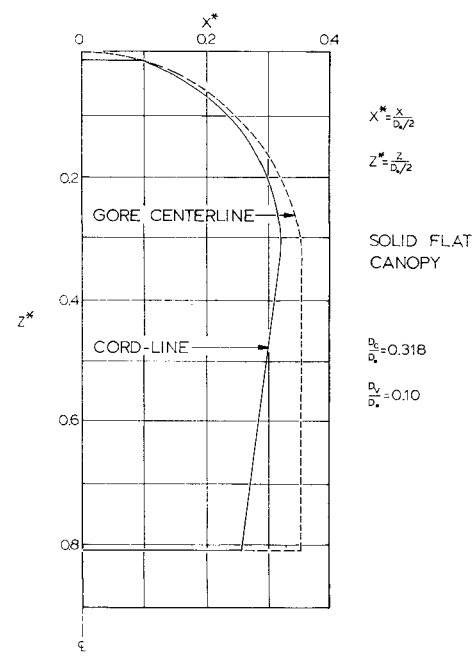

Fig. 10 Profile shape of rigid model 3.

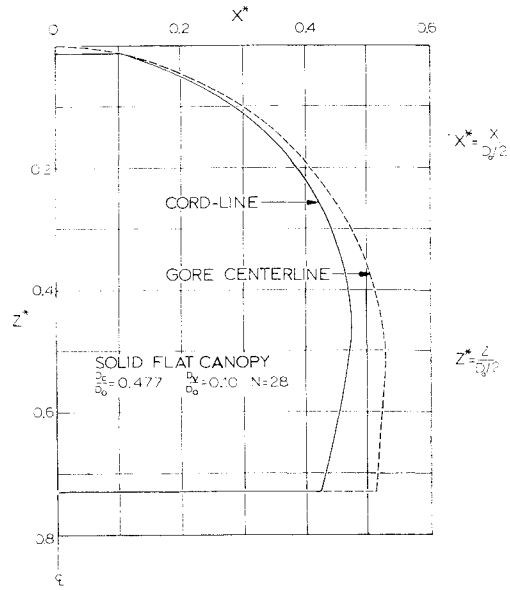

Fig. 11 Profile shape of rigid model 5.

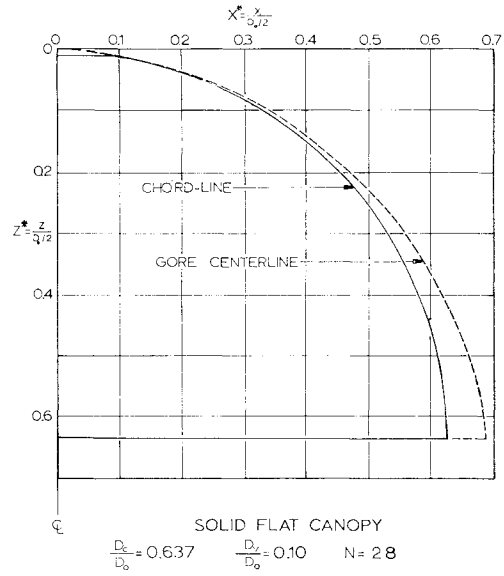

Fig. 12 Profile shape of rigid model 7.

magnitude of the strain involved in Eq. (19a), and an iteration process can be performed until Eq. (19a) is satisfied.

4) After ϵ is known, the stress can be calculated from Eq. (17).

V. Illustrative Example

In order to illustrate the application of the present method, the stress distribution of a parachute will be calculated whose opening characteristics have been determined through wind-tunnel experiments. This parachute model represents a solid flat canopy having 28 gores. The specifications of this type of parachute are indicated below:

number of gores, $N = 28$
nominal diameter, $D_0 = 3$ ft
canopy area, $S_0 = 7.06$ ft^2
canopy material = 1.1 oz nylon, MIL-C-7020B
modulus of elasticity, $E = 2180$ lb/ft, Ref. 8
vent diameter, $D_v/D_0 = 0.10$
straight cut gores

The most important opening characteristics of a parachute are its instantaneous speed and projected diameter, both considered with respect to time. For this particular model, these characteristics are represented in Figs. 7 and 8. Related to the diameter-time relationship in Fig. 8 are the profile drawings presented in Figs. 9–12. These are correlated to the sequence of the O'Hara shapes shown in Fig. 1. Thus, the opening shock experiments in the wind tunnel provided the correlation between the shape and velocity histories. With the shape-velocity-time correlation, one can establish the instantaneous dynamic pressure q_∞, which provides the necessary numerical information related to the pressure distributions as indicated in Fig. 1. With this aerodynamic background information established, the stress analysis may proceed as follows.

Figures 9–12 represent the cord profiles from which the profile of the gore centerline can be calculated in accordance with Eqs. (7a, 9a, and 14a).

It should be noticed that this procedure is the reverse of the one described in Sec. IV, since here the profiles of the cords are assumed to be known, and the gore profiles are being calculated. All of the established equations are valid, and one has to find merely the relationship between s_g^* and s_c^* which amounts to

$$s_g^* = s_c^*[\cos(\pi/N)] \tag{23}$$

With s_c^* and s_g^* known, Eq. (7a) or (9a) can be solved, whichever is applicable.

For further convenience in the calculation, the pressure distribution of the various shapes as shown in Ref. 8 has been replotted as a function of the cord length s_c^*. The results are shown in Fig. 13.

Knowing the instantaneous dynamic pressure, the parameter λ^* can be calculated for each shape. This has been done, and the results are shown in Fig. 14.

In view of the correlation between λ^* and the strain ϵ as shown in Eqs. (19a) and (20a), the strain distribution of the various models can be calculated, the results of which are shown in Fig. 15.

Under the assumption of perfect elasticity, the stress is merely a multiple of the strain, and the strain presentation may be taken as characteristic for the stress distribution.

The strain curve can now be evaluated for various purposes. For example, one may want to establish the magnitude and location of the maximum stress during the process of opening. The strain curves also reveal that, particularly in the early stages, the strain or stress is highest in the central portion of the canopy. Furthermore, one will notice that the point of the highest strain moves toward the skirt of the canopy as the inflation process approaches its completion. In the case of opening stage no. 1, the strain even reverses theoretically to negative values, which is a consequence of the pressure distribution of this idealized stage showing a resulting pressure from the outer to the inner surface.[8]

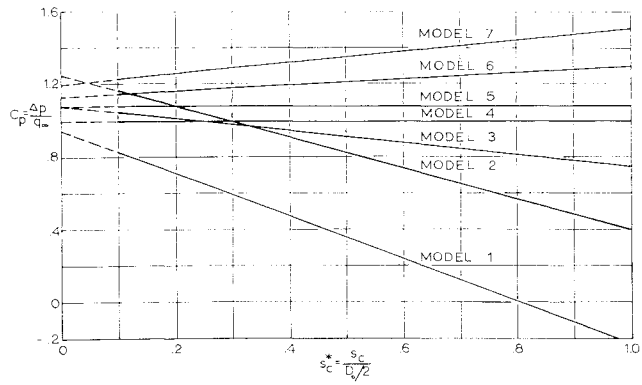

Fig. 13 Pressure coefficient vs canopy location for rigid models 1–7.

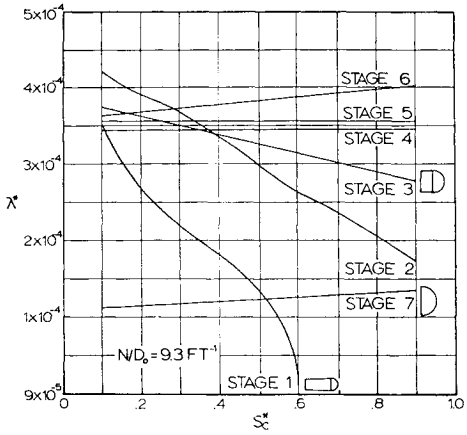

Fig. 14 The dimensionless parameter λ* vs canopy location for seven opening stages of the flexible model.

In concluding this discussion, one should realize that the present method assumes that all of the canopy cloth bulges outwardly between the suspension lines in circular arcs. This is certainly a very questionable assumption, particularly for the skirt region during the early stages of inflation, and one may consider the calculated stresses near the skirt as somewhat unrealistic. However, in the center portions of the canopy, where one may assume a regular bulging of cloth, this assumption is quite good. For the same reason, the stress calculation concerning the portions near the skirt become more realistic as the canopy approaches its state of full inflation.

In view of these facts, one could limit the presented stress calculations to the more central portions of the canopy, particularly for the early stages of inflation. As the inflation progresses, one should extend the calculation gradually toward the skirt portion of the canopy. This method would save time and would probably be satisfactory.

It is evident that a stress analysis always should be coupled with information concerning the dynamics of the parachute opening. This information can be obtained either experimentally or through an opening shock calculation. In case of an experimental approach, one has to record the velocity, force, and size history. This method was essentially employed in the presentation of the illustrative example.

If such suitable experimental data are not available, which is always the case in the design of a new parachute, a rigorous opening shock analysis that also incorporates the effect of apparent mass, apparent moment of inertia, effective porosity, etc., provides the same background information.

In any case, the opening dynamics and the stress analysis are intimately coupled, and this part of the total stress analysis is only as good as the terms and functions representing the dynamics of the opening parachute.

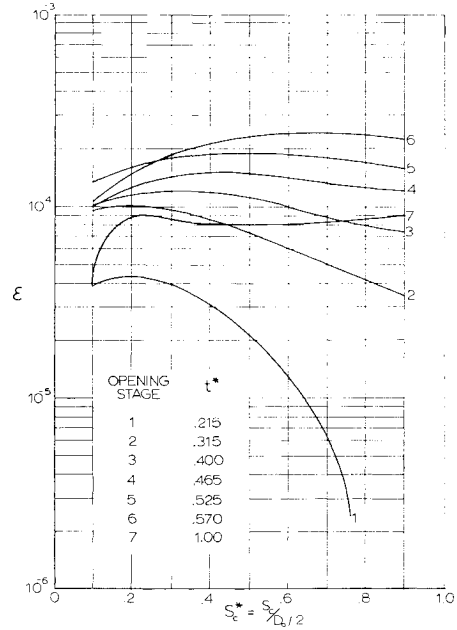

Fig. 15 Strain distribution on the canopy at various stages of inflation.

References

[1] Jones, R., "On the aerodynamic characteristics of parachutes," R&M 862, Aeronautical Research Committee (June 1923).

[2] Stevens, G. W. H. and Johns, T. F., "The theory of parachutes with cords over the canopy," R&M 2320, Ministry of Supply, Aeronautical Research Council (1949).

[3] Duncan, W. J., Stevens, G. W. H., and Richards, G. J., "Theory of the flat elastic parachute," R&M 2118, Ministry of Supply, Aeronautical Research Council (1942).

[4] Beck, E., "The parachute considered as a flexible shell of rotation," U. S. Air Force Transl. F-TS-3630-Re-BR-281 of German Rept. ATI 32297 (November 1942).

[5] Reagan, J. F., "A theoretical investigation into the dynamics and stress analysis of parachutes for the purpose of determining design factors," Daniel Guggenheim Airship Institute Rept. 130 (February 1945).

[6] Topping, A. D., Marketos, J. D., and Costakos, N. C., "A study of canopy shapes and stresses for parachutes in steady descent," Wright Air Development Center TR 55-294, Goodyear Aircraft Corp. (October 1955).

[7] O'Hara, F., "Notes on the opening behavior and the opening forces of parachutes," J. Roy. Aeronaut. Soc. **53**, 1053–1062 (1949).

[8] "Performance of and design criteria for deployable aerodynamic decelerators," Aeronautical Systems Div. ASD-TR-61-579 (December 1963).